phys. stat. sol. (a) **195**, No. 1, 178–182 (2003) / **DOI** 10.1002/pssa.200306286

Influence of lateral patterning geometry on lateral carrier confinement in strain-modulated InGaAs-nanostructures

U. Zeimer[*,1], **J. Grenzer**[2], **S. Grigorian**[2], **J. Fricke**[1], **S. Gramlich**[1], **F. Bugge**[1], **U. Pietsch**[2], **M. Weyers**[1], and **G. Tränkle**[1]

[1] Ferdinand-Braun-Institut für Höchstfrequenztechnik, Albert-Einstein-Str. 11, 12489 Berlin, Germany
[2] Institut für Physik, Universität Potsdam, Am Neuen Palais 10, 14415 Potsdam, Germany

Received 10 September 2002, accepted 30 September 2002
Published online 17 January 2003

PACS 61.10.Kw, 68.35.Gy; 68.65.Fg, 78.55.Cr

Lateral patterning of a tensily strained InGaP stressor layer is used to induce a lateral carrier confinement in an InGaAs-single quantum well (SQW) by lateral strain modulation. It is shown that the value of the induced strain can be influenced by the geometry of the patterned structure. Finite element calculations (FEM) of the strain distribution predict a maximum value of strain for a nearly triangular structure, whereas the strain variation decreases with the valley width of a trapezoidal structure. Samples with different stressor geometry were prepared by holographic photolithography and subsequent wet chemical etching. The optical properties were studied by 10 K photoluminescence (PL). The largest wavelength shift was observed for the sample with the triangular structure confirming the predictions of FEM calculations.

Introduction The problem of lateral confinement attracted much interest in recent years, since device parameters can be altered by an additional degree of freedom. To achieve a lateral carrier confinement, different concepts have been used like self-organized growth of three-dimensional islands [1] or lateral etching through a quantum well (QW) structure followed by subsequent regrowth [2]. Another way to obtain it is to influence the lateral band structure of a QW by a lateral modulation of strain, which is realized by lateral patterning of a stressor layer [3].

In our previous studies [4, 5] we have shown that a lateral carrier confinement inside an InGaAs-single quantum well (SQW) is achieved by lateral patterning of an InGaP stressor layer grown on top of it. The lateral strain modulation which penetrates into the InGaAs-SQW is caused by the lattice relaxation at the free InGaP surfaces and gives rise to a periodic change of the lateral band structure. The sign of the strain in the stressor layer, i.e. positive (tensile strain) or negative (compressive strain) defines the photoluminescence (PL) peak shift of the QW emission after patterning compared to the unpatterned sample. For this experiment we used the same absolute amount of strain in the InGaP stressor layer, i.e. 0.3% and the same geometry of patterning. We obtained a blue shift of the PL wavelength of the InGaAs-QW for compressive strain in the stressor layer and a red shift for the tensily strained stressor. However, the wavelength shift was only about 10 meV compared to the unpatterned sample. In order to increase the PL wavelength shift, in this paper we report on the influence of the patterning geometry of the stressor layer, i.e. the ridge to valley ratio, on the strain distribution and the optical properties of the SQW.

[*] Corresponding author: e-mail: zeimer@fbh-berlin.de, Phone: +49 30 63922679, Fax: +49 30 63922685

 0031-8965/03/19501-0178 $ 17.50+.50/0

Information about the two-dimensional strain distribution is obtained theoretically by finite element calculations (FEM) and experimentally by grazing incidence X-ray diffraction (GID). The optical properties of the InGaAs-SQWs are studied by 10 K photoluminescence (PL).

Experimental The samples were grown by low pressure metalorganic vapour phase epitaxy (MOVPE) at 600 °C on exactly oriented (001) GaAs substrates. The common precursors trimethylindium (TMIn), trimethylgallium (TMGa), arsine and phosphine were used. After deposition of a 100 nm thick GaAs buffer layer the 10 nm thick $In_xGa_{1-x}As$-SQW with $x = 0.16$ ($\varepsilon = -1.14\%$) was grown followed by a 10 nm thick GaAs layer which serves as barrier and etch stop layer. After this the 120 nm thick tensily strained ($\varepsilon = 0.3\%$) InGaP stressor layer and the 10 nm thick GaAs cap layer were grown. The vertical layer sequence was checked by high resolution X-ray diffraction (HRXRD) using a Philips MRD. The experimental rocking curves were fitted with the SmoothFit program confirming the target values.

The preparation of the lateral pattern was done by holographic photolithography using a positive photoresist followed by subsequent wet chemical etching. Details are described elsewhere [6]. By wet chemical etching a trapezoidal surface grating with nearly {111} sidewalls and a period of either 1000 or 500 nm is produced. Ridges and valleys run parallel to the [1–10] direction. In the valleys the InGaP was completely removed down to the GaAs etch stop layer. By varying the exposure contrast, the etching time and the grating period different valley widths ranging from 240 nm down to 0 (triangular shape) could be achieved.

PL spectra were recorded at 10 K by using a HeNe laser with an incident power of 4 mW as excitation source. The laser spot was focused down to a diameter of 0.2 mm. For the detection of the spectra a 1 m monochromator and a photomultiplier tube were used. To study the temperature dependence of the spectra the sample temperature was increased in steps of 10 K up to 150 K.

To characterize the depth distribution of the strain in the structure we used the grazing incidence X-ray diffraction (GID) method [7]. The measurements were carried out at beamline ID 10B at the European Synchrotron Radiation Facility (ESRF) in Grenoble using a monochromized X-ray beam with a wavelength of 0.1548 nm. Scans were performed in reciprocal space using a coordinate system rotated by 45 degrees around the [001] surface normal compared to the usual cubic coordinate system. By using a Si-analyzer in front of the detector a resolution in reciprocal space of better than 2×10^{-4} nm^{-1} could be achieved. Scans measured at the (200) reflection (equivalent to (220) reflection in cubic coordinates) are sensitive to in-plane strains in our structure. The depth information about the strain is obtained by varying the incidence angle α_i of the incoming X-ray-beam. By this method the change in the in-plane lattice parameter a_{II}, i.e., the so-called total strain ε_T is measured.

Results and discussion In Fig. 1 scanning electron microscopy (SEM) pictures of the cleaved edges of two typical samples are shown. It is seen, that nearly {111} sidewalls could be achieved. Inside the valleys the etch process stopped at the GaAs etch stop layer. That was confirmed by transmission electron microscopy investigations and means, that also inside the valleys still a barrier exists for the carriers that are introduced into the InGaAs-QW.

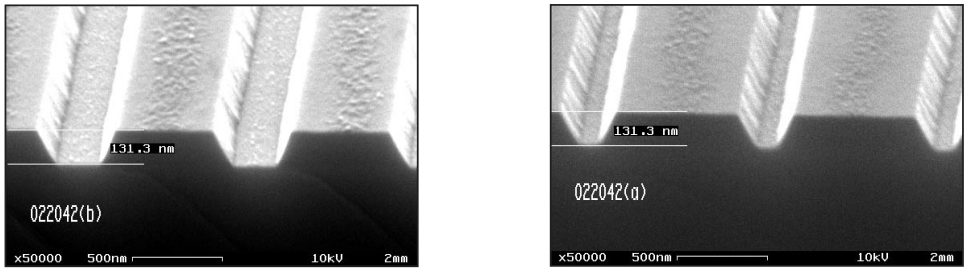

Fig. 1 SEM pictures of surface gratings with a period of 1000 nm for sample 1 (left-hand side, valley width = 240 nm) and sample 2 (right-hand side, valley width = 95 nm).

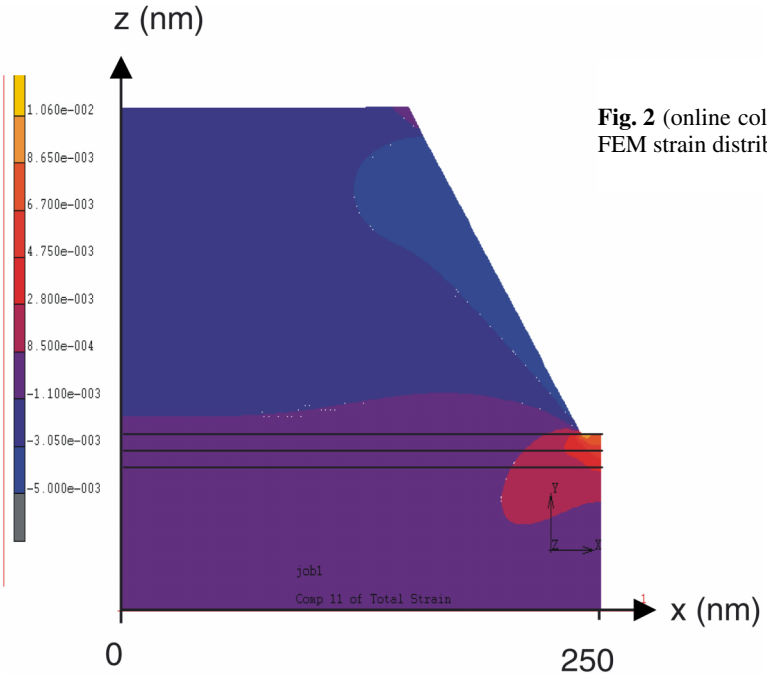

Fig. 2 (online colour at: www.interscience.wiley.com) FEM strain distribution map.

For the theoretical prediction of the strain distribution from the geometrical sample parameters (vertical layer structure as well as lateral geometry of the surface grating) of the samples we used FEM calculations. In Fig. 2a typical map of the total strain distribution ε_τ is shown. Orange colour is attributed to tensile strain, whereas blue colour represents compressive strain. Violet colour corresponds to zero strain (mainly seen in the substrate). The positions of the InGaAs-QW and the GaAs etch stop layer are indicated. The calculation is done for 500 nm grating period. Beneath the valley a tensily strained region is seen that penetrates also into the substrate. The blue colour in the InGaP region indicates some small compressive strain caused by the relaxation at the free surfaces. For a 1000 nm grating period this compressive strain vanishes in the middle of the ridge, but for a 500 nm period an overlap of the strain fields for adjacent ridges takes place. By reducing the grating period further this overlap becomes stronger and therefore the absolute value of the tensile strain beneath the valleys becomes smaller.

Results of the GID measurements for samples 1 and 2 are presented in Fig. 3. In all scans shown in Fig. 3 intensity oscillations with a high frequency are observed caused by the one-dimensional lattice of

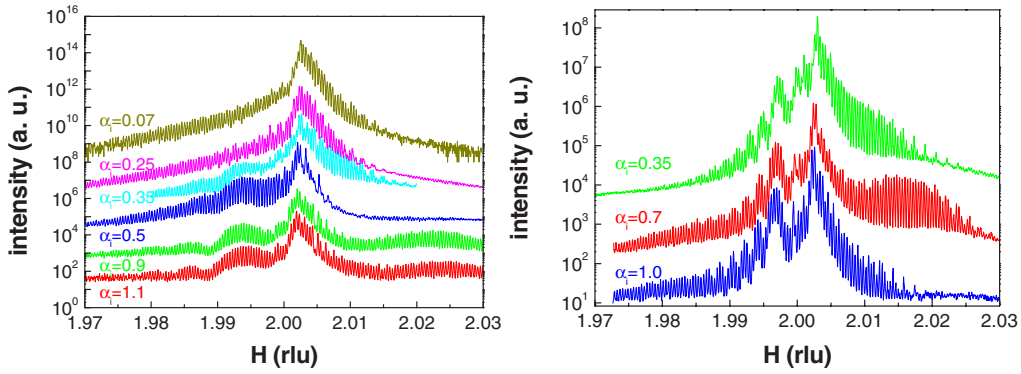

Fig. 3 (online colour at: www.interscience.wiley.com) GID-scans for different α_i values at (200) reflection for sample 1 (left-hand side) and sample 2 (right-hand side).

Table 1 Strain values obtained from GID-scans.

sample	valley width (nm)	$\varepsilon_\tau^{\,1}$	$\varepsilon_\tau^{\,2}$	w (nm)
1	240	0.15%	−0.12%	195
2	95	0.31%	−0.10%	76

the surface grating. From the difference of the H-values of two neighbouring oscillations the grating period can be calculated (in this case 1000 nm). For sample 1 the shape of the intensity pattern changes significantly with the incidence angle α_i. For $\alpha_i = 0.07°$ the X-ray beam penetrates only about 10 nm into the sample. Thus from this scan information is obtained mainly about the GaAs cap layer. If there was no in-plane lattice parameter change compared to the GaAs substrate, the intensity maximum should be located at $H = 2.0$. But the intensity maximum is shifted to a higher H value indicating a smaller in-plane lattice constant compared to GaAs. This can be caused by the fact, that the material near the free InGaP sidewalls of the ridges can relax to its own lattice parameter. Since the InGaP was pseudomorphically tensily strained, its free lattice constant is smaller than GaAs. That means, here we measure the in-plane lattice constant of the relaxed part of the former tensily strained InGaP, which is also induced into the thin GaAs cap layer. For larger α_i, i.e. increasing penetration depth, the relaxed region near the surface always contributes to the signal. Thus, in all scans a local intensity maximum appears at the same value $H > 2$. For $\alpha_i \geq 0.35°$ a second local intensity maximum appears on the left hand side ($H < 2$). The information depth approaches the region of the InGaAs-QW. Since the in-plane lattice parameter a_{II} in this case is larger than for GaAs, the additional maximum is caused by tensile strain near the QW. We relate this feature to the tensily strained region beneath the valley predicted from the FEM calculations (see Fig. 2).

The H-scans for sample 2 show similar behaviour. At $\alpha_i \geq 0.35°$ the same two local intensity maxima can be seen, but the intensity of the one located at $H < 2$ is much larger and the H-value difference to $H = 2$ is smaller compared to sample 1. Additionally this local intensity maximum is accompanied by side maxima similar to thickness fringes in rocking curves. This seems to be a measure for the width of the strained region. Since the only difference between the two samples is the ridge/valley ratio, it can be concluded, that the tensily strained region near the InGaAs-QW is larger for sample 2, but the strain is smaller. In Table 1 for both samples the strain values and the width of the strained region w, calculated from the H-values, are listed.

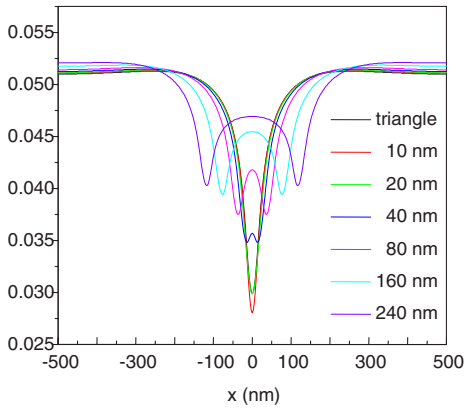

Fig. 4 (online colour at: www.interscience.wiley.com) Band edge shift due to lateral strain.

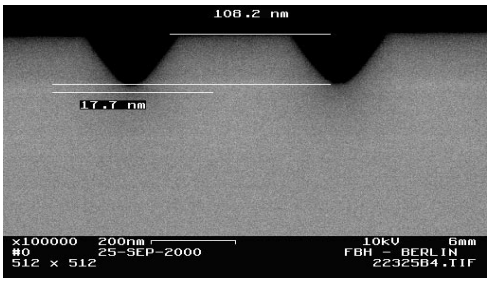

Fig. 5 Nearly triangular structure with 500 nm period (sample3).

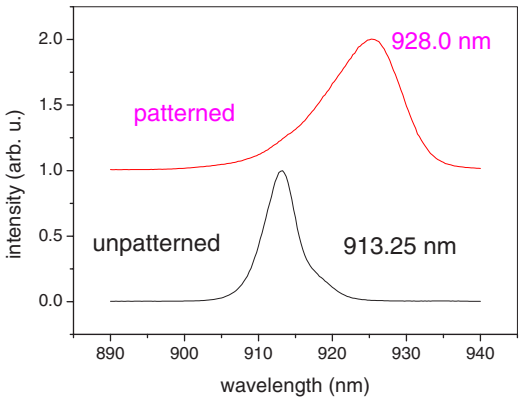

Fig. 6 (online colour at: www.interscience.wiley.com) 10 K PL spectra for sample 3.

It is seen, that ε_τ^1, which is attributed to the region beneath the valley, differs significantly indicating a strong strain dependence on the valley width (or ridge/valley-ratio), whereas ε_τ^2 is almost identical. Since material and pseudomorphic strain in the InGaP are identical for both samples, the relaxation on the free InGaP sidewalls leads to a similar lattice constant a_{II}.

From the FEM strain distribution the lateral band structure can be calculated [4, 5]. The results for different valley widths are shown in Fig. 4. For the given vertical layer sequence the highest band edge shift of 25 nm is obtained for a valley width of 10 nm.

Using this prediction we tried to prepare a nearly triangular structure. This could be realized only for a grating period of 500 nm (sample 3, Fig. 5). For sample 3 from GID measurements $\varepsilon_\tau^1 = 0.5\%$ was determined being considerably higher than for samples 1 and 2. All three samples were measured by 10 K PL. The wavelength shift compared to the unpatterned sample amounts to 8, 12 and 22 meV for samples 1, 2 and 3, respectively (Fig. 6). This results are in excellent agreement with the predictions from band structure calculations. For sample 3 the temperature dependence of the wavelength shift was studied. The wavelength shift becomes smaller at higher temperatures, but the effect can be observed up to 150 K.

Conclusions It could be shown that the lateral geometry of the surface grating which is etched into an InGaP stressor layer on top of an InGaAs-QW has a large influence on the three dimensional strain distribution. From FEM calculations of the strain distribution an optimal lateral geometry, namely a nearly triangular structure, was found. The calculated strain values for the different geometries were verified by GID measurements. The predictions from band structure calculations on the basis of the strain distribution agree very well with the experimentally obtained PL results. This approach can be used for further optimisation of the vertical and lateral sample geometry in order to obtain a wavelength shift even larger than the 22 meV observed for this series of samples.

Acknowledgement The authors thank the Deutsche Forschungsgemeinschaft for financial support of the work under contract No. Tr 357 and Pi 217.

References

[1] D. Bimberg, M. Grundmann, and N. N. Ledentsov, Quantum Dot Heterostructures (Wiley, Chicester, 1998).
[2] B. P. van der Gaag and A. Scherer, Appl. Phys. Lett. **56,** 481 (1990).
[3] K. Kash, J. M. Worlock, D. M. Sturge, P. Grabbe, J. P. Harbinson, A. Scherer, and P. S. D. Lin, Appl. Phys. Lett. **53**, 782 (1988).
[4] U. Zeimer, J. Grenzer, U. Pietsch, S. Gramlich, F. Bugge, V. Smirnitski, M. Weyers, and G. Tränkle, J. Phys. D **34**, A183 (2001).
[5] U. Zeimer, F. Bugge, S. Gramlich, V. Smirnitski, M. Weyers, G. Tränkle, J. Grenzer, U. Pietsch, G. Cassabois, V. Emiliani, and Ch. Lienau, Appl. Phys. Lett. **79**, 1611 (2001).
[6] N. Darowski, U. Pietsch, U. Zeimer, V. Smirnitski, and F. Bugge, J. Appl. Phys. **84**, 1366 (1998).
[7] A. Ulyanenkov, N. Darowski, J. Grenzer, and U. Pietsch, Phys. Rev. B **60**, 16701 (2000).